Fabrication of Novel Bio-Adsorbent And Its Application For The Removal of Cu(II) From Aqueous Solution

Dianjia Zhao (dianjia0000@163.com)
Wuhan Institute of Technology https://orcid.org/0000-0002-3245-3624
Wenkang Ye
Wuhan Institute of Technology
Wenxuan Cui
Wuhan Institute of Technology

Research Article

Keywords: Hydroxyapatite, Adsorption, Sodium alginate, Cellulose, Heavy Metal, bio-adsorbent

Posted Date: July 12th, 2021

DOI: https://doi.org/10.21203/rs.3.rs-606332/v1

Version of Record: A version of this preprint was published at Environmental Science and Pollution Research on October 18th, 2021. See the published version at https://doi.org/10.1007/s11356-021-17013-4.

Fabrication of novel bio-adsorbent and its application for the removal of Cu(II) from aqueous solution

Dianjia Zhao*, Wenkang Ye, Wenxuan Cui

Key Laboratory for Green Chemical Process of Ministry of Education, School of Chemical Engineering and Pharmacy, Wuhan Institute of Technology, Wuhan, 430073, China

*Corresponding author 1: Dianjia Zhao, Tel: 86-15221702905

E-mail address: dianjia0000@163.com

Abstract

As an eco-friendly adsorption material, hydroxyapatite (Ha) have received widely attention from researchers owing to their excellent biocompatibility and adsorption performance. However, the inconvenient in separating Ha powder from adsorbed processes following use has limited their application. Herein, a novel alginate-based composite beads encapsulation with cellulose and Ha (named HCA) was designed to remove Cu(II) from aqueous solution. Fourier-transform infrared spectroscopy (FTIR), X-ray diffraction (XRD), Scanning electron microscopy (SEM), and X-ray photoelectron spectroscopy (XPS) were used for characteristic analysis. The impacts of samples compositions, various Cu(II) concentration, adsorption equilibrium time, and regeneration performance on the adsorption process were investigated. The results suggested that beads exhibited their maximum adsorption capacity for Cu(II) was obtained to be 64.14 mg/g at pH=5 for 8 h, best fitted into Langmuir isotherm models and the pseudo-second-order kinetic model. In addition, the biocompatible beads not only increase the sorption sites, but also have good regenerability, would be a promising bio-adsorbent for heavy metal ion removal.

Keywords : Hydroxyapatite; Adsorption; Sodium alginate; Cellulose; Heavy Metal, bio-adsorbent.

Introduction

Attendant with the growth of global industrialization and urbanization, water environment such as lakes and river have been polluted by human-mediated activities. Emission of heavy metals has raised increasing concern, due to their toxicity, carcinogenicity, and non-biodegradable in living organisms. To address the problem of water pollution, many efficient strategies were used for the separation and purification of contained water, such as chemical precipitation(Ebrahimi et al. 2017), membrane filtration(Jiang et al. 2018), electrochemical treatment and adsorption-based separation (Shalla et al. 2019). Among these various techniques, adsorption is effective and widely used in water treatment because of the facile and low-cost operation (Joseph et al. 2019). Various adsorbents have been evaluated, including graphene oxide (GO), and metal organic frameworks (MOF) (Zhu et al. 2019; Yap et al. 2020). However, the inconveniently in separating these powder materials after adsorption process limit their application for water treatment.

Sodium alginate (SA), a polyanionic polymer, can crosslink with divalent metal ions to form a stable framework with three-dimensional (3D) network structure, which can combined with nanomaterials to overcome the barrier in separation and recover of nanomaterials after adsorption process (Song et al. 2019). Futhermore, their surface with hydroxyl and carboxyl groups provide large amounts of bonding sites, which are conducive to capturing metal ions. For instance, Baigorria et al. introduced bentonite-composite polyvinyl alcoho into the network structure of composite hydrogel beads, forming adsorbents that are stable and with excellent

adsorption performance for As (Baigorria et al. 2020). Considering the interdependency of the physical and chemical properties of alginate-based hydrogels, the powder material encapsulated into the hydrogel network not only outstanding change its structure, but also could enhanced in environmental applications (Lva et al. 2019). Accordingly, Ha is a natural mineral calcium apatite, which is the main component of hexagonal crystal of calcium, phosphorus and oxygen(Szcześ et al. 2017). Due to its nontoxicity, high adsorption efficiency, high biocompatibility and cost-effective production, Ha may be an alternative material for heavy metal removal.

Recently, bioadsorbents have attracted more and more attention because of their non-toxic and biodegradable properties (Muya et al. 2016). Natural biopolymers (e.g., cellulose, pectin and chitosan), as a biodegradable, abundant, and renewable resource, has attracted great attention for the design of sorbent materials from security concern. Cellulose is considered to be renewable polysaccharide and widely in the world. In the long run, non-poisonous, ecological, and abundant bio-polymers will be undoubtedly beneficial for supplying clean water for the human (Zhang et al. 2020). More important, Cellulose can form a stable network structure through physical crosslinking, which is helpful to provide more adsorption sites. In the past years, some researchers have employed cellulose composite beads to improve their adsorptive properties for heavy metal removal of from wastewater (Luo et al. 2016; Liu et al. 2020).

Inspired by the advantages alginate and cellulose based material, we develop a nontoxic and eco-friendly bio-adsorbent for the removal of heavy metal ion (Cu(II))

from aqueous solution. The fabrication of the adsorbent was described in Scheme 1. We hypothesized that if the good adsorption performance of Ha could be combined with the good 3D porous performance of cellulose and alginate material, the difficulty of separation of ha from water can be overcome, the adsorption performance of hydrogel beads could be improved. The adsorbent performance was evaluated in view of the adsorption kinetics, isotherms and thermodynamics. The outcomes of our study suggest that the cross-linked HCA composite beads are a potential adsorbent for efficient water purification.

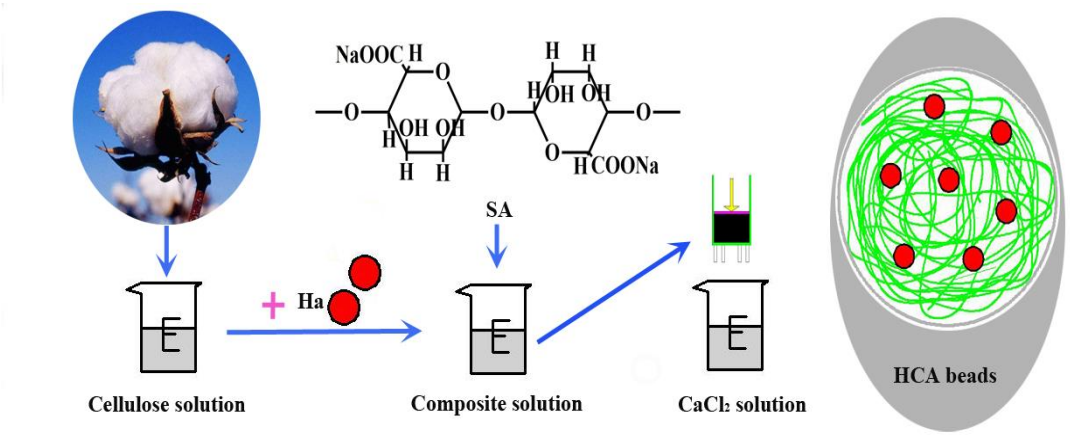

Scheme 1. Schematic diagram for the characterization of HCA beads

2.Methods and Materials

2.1 Materials

Cellulose (α-cellulose) was kindly obtained by Hubei Golden Ring Co.,Ltd. (Xiangyang, China). Sodium hydroxide (NaOH), urea, sodium alginate, copper sulfate pentahydrate ($CuSO_4.5H_2O$) and calcium chloride were provided by Sinopharm Chemical Reagent Co., Ltd (Shanghai, China). Ha (≥97%, <100nm) was obtained from Aladdin industrial corporation (Shanghai, China). Deionized (DI) water was

91 supplied from a TS-DI water filtration system.

92 2.2 Preparation of the cellulose solution (CS)

93 Cellulose (4g) was rapidly dissolved into NaOH/urea/H_2O(7:12:81, weight ratio)
94 solution at low temperature condition (-12 ℃) according to the reported method (Qi
95 et al. 2009). The resulting solution stirring for 5 min, until to obtained the transparent
96 CS.

97 2.3 Preparation of the HCA beads

98 Firstly, the Ha (0.1 g, 0.2 g, 0.4 g, 0.8 g and 1.6 g) and CS (0.2 g, 0.4 g, 0.8 g, 1.6
99 g and 3.2 g) were added into SA solution (1%, w/v), respectively. The mass ratios
100 (Ha:CS:SA) of mixed solution for (0.1:0.2:1) (0.2:0.4:1) (0.4:0.8:1) (0.8:1.6:1) and
101 (1.6:3.2:1). Then, the mixture were stirred for 0.5 h to produce mixed solution evenly.
102 Finally, the mixed solution was dropped into $CaCl_2$ solution (2%, 200 mL) using a 20
103 mL syringe. After curing for 6 h, the obtained HCA beads were washed three times
104 with deionized water.

105 2.4 Adsorption Investigation

106 To systematically study Cu(II) adsorption behaviors of HCA beads, adsorption
107 experiments were conducted using Cu(II) as model heavy metal ions. An optimized
108 dose of wet adsorption beads were added to 50ml of copper ion solution, the
109 concentrations of the initial solutions were 100-500mg/L. Therein, it is ensured that
110 adsorbents has well contact with the solution, the concentration of the adsorbed
111 solution was determined by spectrophotometry (Apha 2005). the results were repeated
112 for three times. Adsorption capacity was calculated using the following equation:

$$q_e = \frac{(Co - Ce)\ V}{\mathrm{m}} \quad (1)$$

The removal rate of Cu(II) by HCA was calculated from each step and defined as:

$$R\text{emoval}\ (\%) = \frac{C_0 - C_e}{C_0} \times 100\% \quad (2)$$

q_e stands for the adsorption capacity of the bio-adsorbent for heavy metals (Cu(II)) (mg/g), V is volume of Cu(II) solution (L), and C_0 and Ce are concentration of the initial and equilibrium, respectively.

2.5 Characterization methods

Fourier-transform infrared spectra (FTIR) of the product was performed on a spectrometer (Nicolet 6700). X-ray diffraction (XRD) test of sample was carried out by an XRD Rint-2000 diffractometer. The surface microstructure of the product was observed by a scanning electron microscopy (SEM) Nova Nano SEM 230 with an energy dispersive spectroscopy (EDS) for analyzing different elements. Elemental analysis of the materials was performed on X-ray photoelectron spectroscopy (XPS) ESCALAB 250Xi.

2.6 Regeneration experiment

To further investigate the reusability of HCA beads for Cu(II) adsorption, the desorption experiments were carried out with 0.1mol/L $Ca(NO_3)_2$ solutions, 0.01mol/L HNO_3 and deionized water. After elution, the regenerated HCA beads was subsequently evaluated in adsorption experiments to study their recyclability.

3. Results and discussion

3.1. Characterization of the samples

3.1.1. FT-IR analysis

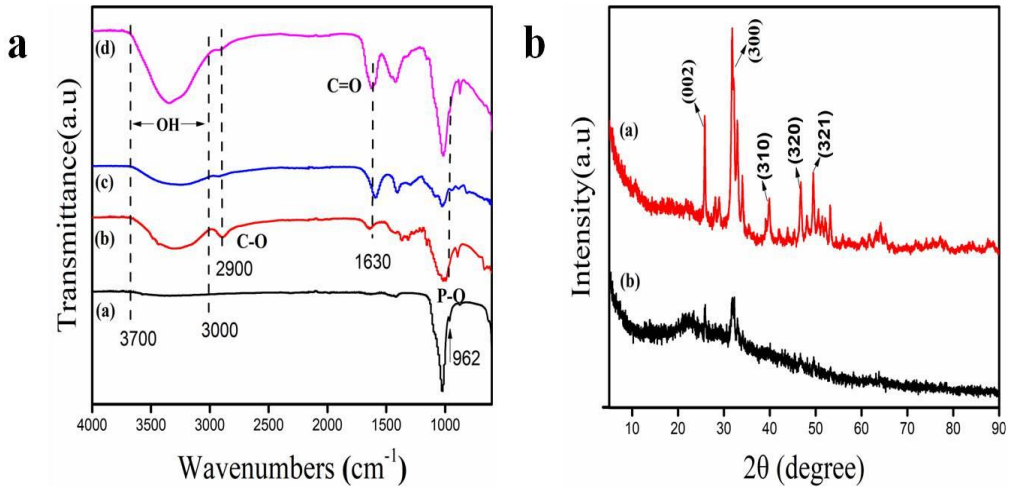

Fig. 1 . a: FTIR spectra of Ha (a), Cellulose (b), CA (c) and HCA(d). b: XRD patterns of Ha (a) and HCA (b)

To investigate the interaction between the Cellulose and Ha, CA and HCA, the prepared sample were characterized by FTIR spectra and XRD patterns. The results were presented in Fig. 1a and Fig. 1b. As shown in Fig. 1a, FTIR analysis show the characteristic absorbance of the Ha (a), CA (b), Cellulose (c) and HCA (d). The absorption peak at around 962 cm^{-1} is derived from stretching modes of P-O in HCA composite beads (Zhang et al. 2019). After the Ha and Cellulose were introduced into CA, the asymmetric and symmetric stretching vibrations of the C=O bands shifted to 1630cm^{-1} (HCA) from 1640 cm^{-1} (Cellulose) and 1590 cm^{-1} (CA), which also provided evidence for the interaction between Cellulose and sodium alginate matrix. These new peak at 2900 cm^{-1} was corresponding to the stretching vibration of C-O, which confirms the binding of cellulose and alginate chains on the HCA surface by the electrostatic force (Luo et al. 2016). A broad absorption peak at around 3600-3000

151 cm^{-1} was derived from the stretching vibrations of hydroxyl groups in the HCA,
152 suggesting the more stronger interaction among the alginate matrix. The XRD
153 patterns of the obtained Ha (a) and HCA (b) are presented in Fig. 1b. The diffraction
154 peaks (002), (300), (310), (320), and (321) can be indexed to $Ca_5(PO_4)_3OH$ (JCPDS
155 09-0432). For HCA composites, the intensities of diffraction peaks of Ha in the XRD
156 pattern decline, indicating the exist of the Ha content in the as-prepared materials.
157 3.1.2 SEM and EDS analysis

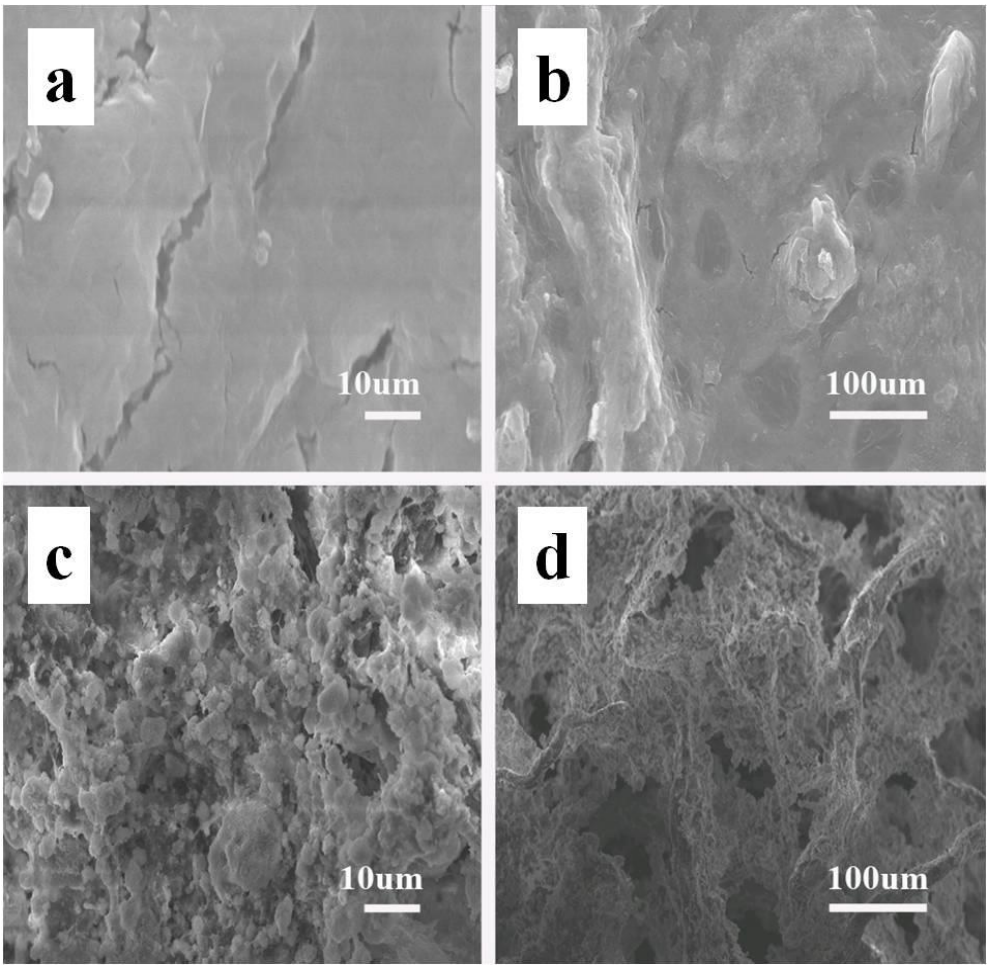

158

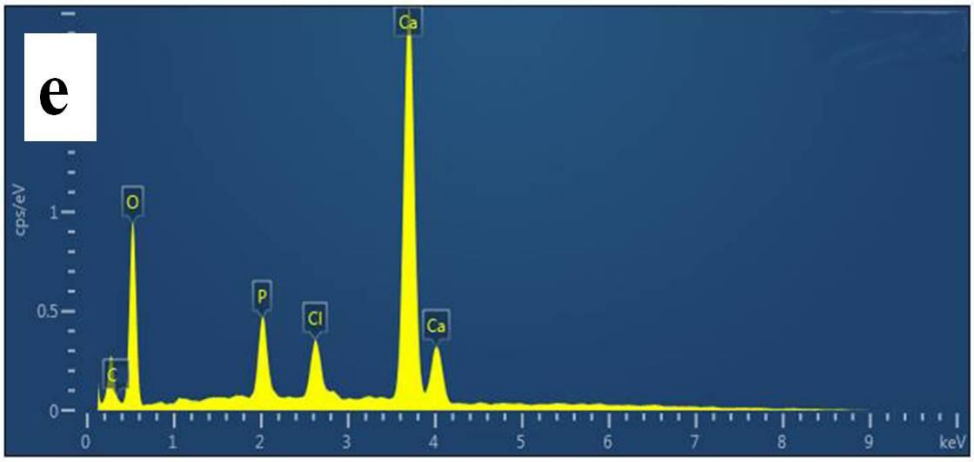

Fig. 2. SEM images of CA and HCA composite beads (a-d), EDS spectra of HCA (e).

As shown in Fig. 2(a-b) we can see that the morphological structure of CA with smooth fracture surface, which may be caused by dehydration of the hydrogel beads. For the HCA composite beads in Fig. 2(c-d), as expected, the surface showed an irregular wrinkled structure, which would be conducive to the adsorption of heavy metal ions. In addition, the composite beads appeared visible huge porous more cavities significantly (Fig. 2d). Hence, the new structure could increase more active sites, which was also beneficial for the adsorption of metal ions onto the HCA material. In this way, the adsorption process of heavy metal ions Cu(II) not only occur on the surface of the bead, but also interact with its internal active sites, thus the adsorption sites can be maximized. In addition. the EDS analysis of HCA show that the composite hydrogel beads is mainly composed of C, O, P, Cl and Ca elements (Fig. 2e), which demonstrated that Ha was successfully encapsulated into Cellulose and alginate-based matrix.

3.1.3 XPS analysis

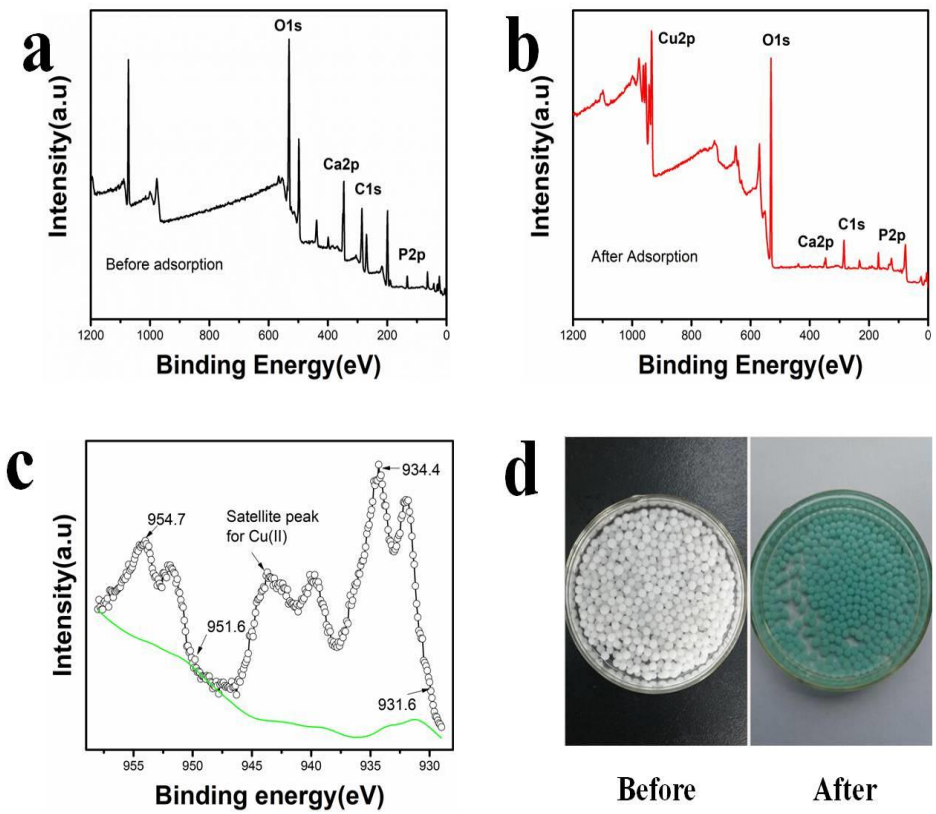

Fig. 3. The XPS survey spectra of HCA before and after Cu(II) adsorption

In order to study the changes of related elements before and after the adsorption of adsorbent, the XPS spectra of Cu(II) adsorption before and after the modification of HCA were analyzed(Fig. 3 a.b). The high resolution energy spectrum shows the elemental composition of the HCA hydrogel beads, and the binding energy signals at 284.8 eV, 347 eV and 532 eV correspond to the $C1_s$ peak, $Ca2_p$ peak and $O1_s$ peak in HCA, respectively (Zhang et al 2020). When Cu(II) was adsorbed, the characteristic peak of $Cu2_P$ appeared, indicating that the heavy metal Cu(II) ion was successfully adsorbed to the surface and/or interior of HCA. For the high-resolution $Cu2_p$ spectra (Fig. 3c), the XPS peak binding energies of Cu $2_{p1/2}$ and Cu $2_{p3/2}$ are 951.6-954.7 eV and 931.6-934.4 eV, respectively (Godiya et al 2019). In addition, the satellite peak is located at the binding energy 944.3 eV (Zhang et al 2020), which also indicates that

188 Cu(II) exists on the surface of HCA hydrogel beads.

189 **3.2 Adsorption studies**

190 3.2.1 Adsorption kinetics of HCA beads

191 In order to further understand the adsorption process, the adsorption experiment
192 was evaluated by the following kinetic model (Bo et al 2020).

193 The pseudo-first-order kinetic Eq. (5):

194 $$Ln(q_e - q_t) = \ln q_e - k_1 t \quad (3)$$

195 The pseudo second-order kinetic Eq. (6):

196 $$\frac{t}{q_t} = \frac{1}{k_2 q_e^2} + \frac{t}{q_e} \quad (4)$$

197 Where, q_e represents adsorption capacity of the equilibrium (mg/g), and q_t
198 represents the adsorption capacity at time t (min). k_1 (L/min) and k_2 (g/mg.min)
199 represents adsorption rate constants.

200 Table 1 Compositions of the prepared HCA beads samples

Samples	HCA-1	HCA-2	HCA-3	HCA-4	HCA-5
HA	0.1%	0.2%	0.4%	0.8%	1.6%
CS	0.2%	0.4%	0.8%	1.6%	3.2%
SA	1%	1%	1%	1%	1%

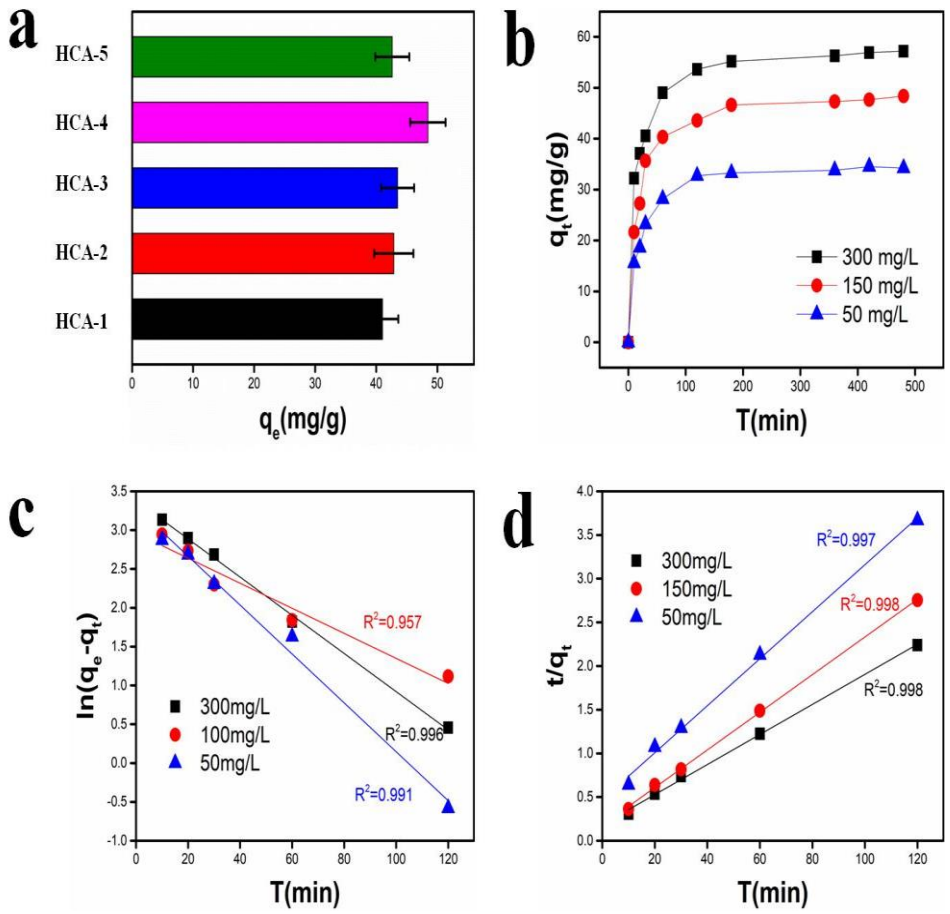

Fig. 4. (a) Effect of the mass ratio of HCA contents for Cu(II) (Temperature: 293 K, pH=5). (b) fitting curves of adsorption kinetics. (c) pseudo-first-order model of HCA beads. (d) pseudo-second-order model of HCA beads.

Table 1 shows the different mass ratios of the HCA samples with Ha, CS, and SA in the preparation process. The influence of different mass ratios of Ha, CS, and SA on the adsorption capacity was also investigated (Fig. 4a). As demonstrated above, considering the adsorption capacity, the optimal mass ratio of Ha/CS/SA was determined to be 0.8% : 1.6% : 1%. In order to investigate their adsorption properties. HCA beads were placed in conical flask containing 50 mg/L, 150 mg/L, and 300 mg/L Cu(II) solution (50 mL, pH=5), respectively. The results are shown in Fig. 4b,

as the increase of Cu(II) concentration, the adsorption capacities of HCA beads obviously increased. The Cu(II) adsorption capacities of the HCA beads reach up to 55.20 mg/g, better than those of other hydrogels materials (Zhang et al 2019, Wu et al 2019). In addition, the experimental results show that the pseudo-second-order kinetic model (300mg/L : R^2=0.998, 150mg/L : R^2=0.998, 50mg/L : R^2=0.997) can better fit the experimental data than the first-order kinetic model (300mg/L : R^2=0.996, 150mg/L : R^2=0.957, 50mg/L : R^2=0.991) for Cu(II) adsorption. The calculated theoretical maximum adsorption capacity is closer to the real experimental value. Therefore, the above results show that the adsorption process of HCA for Cu(II) is more consistent with chemical adsorption (Pu et al 2018).

3.2.2 The isotherm study of HCA

In order to further evaluate the adsorption performance of HCA for Cu(II), Langmuir and Freundlich isothermal models are used to fit the adsorption experimental data. The formula of Langmuir and Freundlich adsorption isothermal model (Kim et al 2017) are:

$$\frac{C_e}{q_e} = \frac{1}{\mathrm{b}q_m} + \frac{C_\mathrm{e}}{q_m} \tag{5}$$

$$lnq_e = lnK_f + lnC_e \tag{6}$$

K (L/mg) represent the Langmuir equilibrium adsorption constant, q_m represent the maximum uptake adsorption capacity (mg/g), C_e represent the concentration (mg/L), and q_e represent the equilibrium adsorption capacity (mg/g) of the two models. n represent a heterogeneous factor.

234 The relevant parameters of Langmuir and Freundlich models are shown in Table
235 2. As you can see from the correlation coefficient R^2, the correlation coefficient of the
236 Langmuir sorption type (R^2=0.990) is higher than that of the Freundlich sorption type
237 (R^2=0.825), indicating that the adsorption type of Cu(II) on HCA beads are more
238 suitable for the Langmuir adsorption isotherm model. Therefore, the adsorption
239 performence of Cu(II) on HCA suggested a monomolecular layer adsorption plays an
240 key role (Hu et al 2018).

241 Table.2 Langmuir and Freundlich adsorption isotherm model parameters for the
242 adsorption of Cu(II) onto HCA at 293 K

T(K)	Langmuir			Freundlich		
	q_m (mg/g)	b(L/mg)	R^2	K_f	n	R^2
303	64.14	0.023	0.990	7.43	2.77	0.825

243

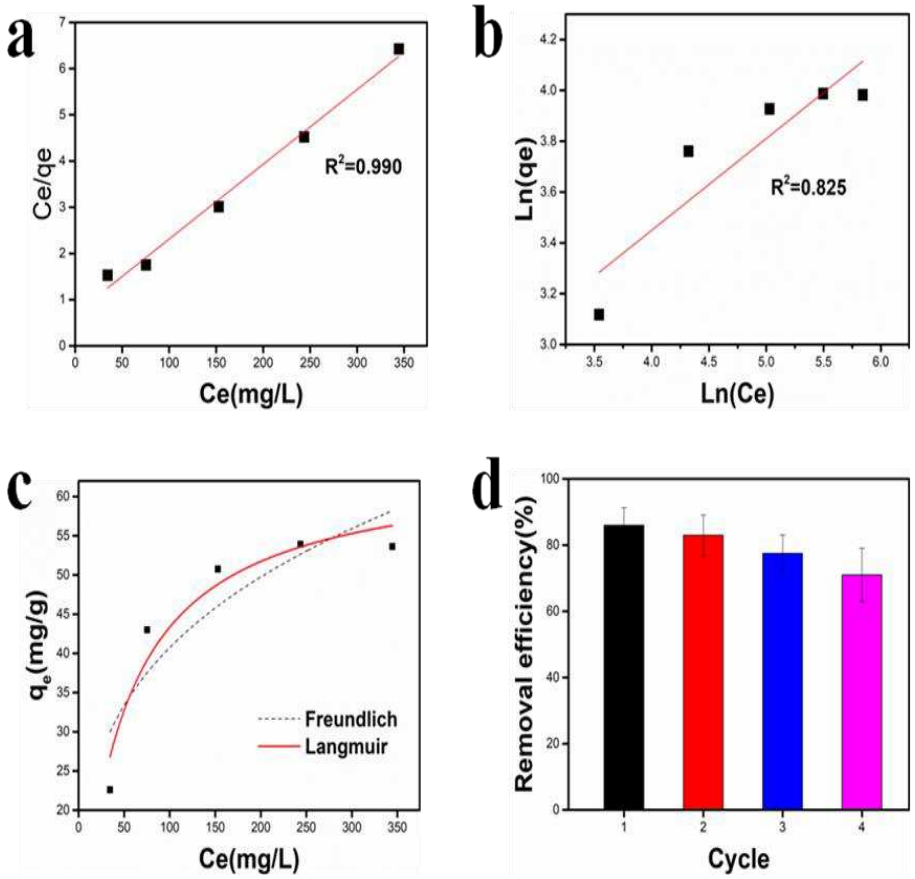

Fig. 5. (a) Langmuir models, (b) Freundlich models, (c) Langmuir isotherm and Freundlich isotherm fitting curve, (d) Reusability of HCA beads for Cu(II) adsorption (30 mg/L, 293 K).

4. Recycling experiment

The regeneration of HCA beads adsorpbents are highly important for further evaluation of its practical application.The material was regenerated in 0.1mol $Ca(NO_3)_2$ and 0.01mol/L HNO_3 solution (Wang et al 2016, Oulguidoum et al 2021). After cleaning with deionized water, the recycled samples were rinsed with distilled water several times to remove trace salt, and then the adsorption test was carried out to study their recycling performance. Fig. 5d shows the relationship between the removal efficiency and the number of cycles. Specifically, after 4 cycles of

experiments, the removal efficiency decreased slightly, but still maintained a good removal efficiency. In conclusion, HCA microbeads not only show good reusability, but also can be separated by gravity, which has potential industrial applications.

5. Mechanisms of Cu(II) removal

The removal of Cu(II) is a complicated process, in which physics and chemistry adsorption might plays an significant role. Specifically, (1) cation-exchange might participate in the adsorption process, namely calcium ions in hydrogel matrix definitely can be replaced with the free Cu(II) ions (Wang et al 2020). (2) The abundance of COO- and O-containing groups on the surface of beads can also easily coordinate with Cu(II) to form complexes (Zhang et al 2020). (3) Besides, Ha possess abundant hydroxyl functional groups, which all help are beneficial for Cu(II) adsorption from wastewater. Therefore, it can be further ascertained that HCA beads have a promising and star candidate for water decontamination.

6. Conclusion

In this study, eco-friendly, micro- and nanostructured and good recycling bio-adsorbent was fabricated via an green cross-linked technology for the removal of Cu(II). The stable surface structure of the adsorbent was confirmed by further FTIR, XRD, SEM and XPS characterization analysis. The adsorption performance were evaluated by using the batch adsorption experiment, and the maximum adsorption capacity of HCA for Cu(II) was 64.14 mg/g, The adsorption kinetics studies showed that the adsorption process for Cu(II) was mainly controlled by chemical adsorption, and Langmuir model fitted the adsorption parameter better. The adsorption-desorption

experiment was repeated for 4 times and still kept a high removal efficiency. In summary, The HCA beads with excellent adsorption performance is promising bio-adsorbent to applications for the removal of Cu(II) from wastewater.

Ethical approval and consent to participate

Not applicable

Consent to publish

Not applicable

Authorship contribution statement

Dianjia Zhao: Conceptualization, Formal analysis, Methodology, Writing - original draft, Validation. Wenkang Ye: Investigation, Visualization, Validation Project administration. Wenxuan Cui: Software, Investigation, Data curation, Writing - review & editing.

Declaration of Competing Interest

The authors declare that they have no known competing financial interests or personal relationships that could have appeared to influence the work reported in this paper.

Funding

The authors gratefully acknowledge financially supported by Sinopec Wuhan Corporation (102049).

Acknowledgements

We thank for Wenkang Ye, Wenxuan Cui helping with the experiment.

Data availability

The datasets used and/or analyzed during the current study are available from the

corresponding author on reasonable request.

References

Apha., 2005 Standard Methods for the Examination of Water and Wastewater, American Public Health Association.

Baigorria, E., Cano, L.A., Sanchez, L.M., Alvarez, V.A., Ollier, R.P. 2020 Bentonite-composite polyvinyl alcohol/alginate hydrogel beads: Preparation, characterization and their use as arsenic removal devices. Environmental Nanotechnology, Monitoring & Management 14, 100364.

Bo, S., Luo, J., An, Q., Xiao,Z., Wang, H., Cai, W., Zhai, S., Li, Z. 2020 Efficiently selective adsorption of Pb(II) with functionalized alginatebased adsorbent in batch/column systems: Mechanism and application simulation. Journal of Cleaner Production 250, 119585.

Ebrahimi, A., Amin, M.M., Pourzamani, H., Hajizadeh, Y., Mahvi, A.H., Mahdavi, M., Rad, M.H.R. 2017 Hybrid coagulation-UF processes for spent filter backwash water treatment: a comparison studies for PAFCl and $FeCl_3$ as a pre-treatment. Environmental Monitoring and Assessment 189, 387-397.

Godiya, C.B., Liang, M., Sayed, S.M., Li, D., Lu. X. 2019 Novel alginate/polyethyleneimine hydrogel adsorbent for cascaded removal and utilization of Cu^{2+} and Pb^{2+} ions. Journal of Environmental Management 232, 829-841.

Hu, T., Liu, Q., Gao, T., Dong, K., Wei, G. & Yao, J. 2018 Facile preparation of tannic acid-poly (vinyl alcohol)/sodium alginate hydrogel beads for methylene blue removal from simulated solution. ACS Omega 3 (7), 7523-7531.

322 Joseph, L., Jun, B., Flora, J. R.V., Park, C. M., Yoon, Y. 2019 Removal of heavy
323 metals from water sources in the developing world using low-cost materials: A review.
324 Chemosphere 229, 142-159.
325 Jiang, S., Zhang, G. Li, Y., Ying, W., 2018 Treatment of natural rubber
326 wastewater by membrane technologies for water reuse, Membrane and Water
327 Treatment 9, 17-21.
328 Kim. H.J., Im. S., Kim. J.C., Hong. W.G., Shin. K., Jeong. H.Y., Hong. Y.J. 2017
329 Phytic Acid Doped Polyaniline Nanofibers for Enhanced Aqueous Copper(II)
330 Adsorption Capability. ACS Sustainable Chemistry & Engineering, 5, 6654-6664.
331 Luo, X., Lei, X., Xie, X., Ning, B.Y., Yu, C. F. 2016 Adsorptive removal of Lead
332 from water by the effective and reusable magnetic cellulose nanocomposite beads
333 entrapping activated bentonite. Carbohydrate Polymers. 151, 640-648.
334 Luo, X., Lei, X., Cai, N., Xie, X., Xue, Y., & Yu, F. 2016 Removal of Heavy
335 Metal Ions from Water by Magnetic Cellulose-Based Beads with Embedded
336 Chemically Modified Magnetite Nanoparticles and Activated Carbon. ACS
337 Sustainable Chemistry & Engineering 4, 3960-3969.
338 Liu, S., Cheng, G., Xiong, Y., Ding, Y., Luo, X. 2020 Adsorption of low
339 concentrations of bromide ions from water by cellulosebased beads modified with
340 TEMPO-mediated oxidation and Fe(III) complexation. Journal of Hazardous
341 Materials 384, 121195.
342 Lva. J., Sun. B., Jin. J., Jiang. W. 2019 Mechanical and slow-released property of
343 poly(acrylamide) hydrogel reinforced by diatomite. Materials Science & Engineering

C-Materials for Biological Applications 99, 315-321.

Muya, F. N., Sunday, C. E., Baker, P. & Iwuoha, E. 2016 Environmental remediation of heavy metal ions from aqueous solution through hydrogel adsorption: a critical review. Water Science and Technology 73 (5), 983-992.

Oulguidoum, A. Bouiahya, K. Bouyarmane, H. Talbaoui, A. Nunzi, J-M. Laghzizil, A. 2021 Mesoporous nanocrystalline sulfonated hydroxyapatites enhance heavy metal removal and antimicrobial activity. Separation and Purification Technology, 255 117777.

Pu, S., Hou, Y., Yan, C., Ma, H., Huang, H., Shi, Q. & Chu, W. 2018 In situ coprecipitation formed highly water-dispersible magnetic chitosan nanopowder for removal of heavy metals and its adsorption mechanism. ACS Sustainable Chemistry & Engineering 6 (12), 16754-16765.

Qi, H.S., Chang, C.Y., Zhang, L., 2009 Properties and applications of biodegradable transparent and photoluminescent cellulose films prepared via a green process. Green Chemistry 11 (2) 177-184.

Shalla, A. H., Yaseen, Z., Bhat, M. A., Rangreez, T. A. & Maswal, M. 2019 Recent review for removal of metal ions by hydrogels. Separation Science and Technology 54 (1), 89-100.

Song, Y., Yang, L.Y., Wang, Y., Yu, D., Shen, J., Ouyang, X. 2019 Highly efficient adsorption of Pb(II) from aqueous solution using amino-functionalized SBA-15/calcium alginate microspheres as adsorbent. Journal of Colloid and Interface Science 125, 808-819.

366 Szcześ, A., Hołysz, L., Chibowski, E. 2017 Synthesis of hydroxyapatite for
367 biomedical applications. Advances in Colloid and Interface Science 249, 321-330.
368 Wang, Z., Wu, S., Zhang, Y., Miao, L., Zhang, Y., Wu, A. 2020 Preparation of
369 modified sodium alginate aerogel and its application in removing lead and cadmium
370 ions in wastewater, International Journal of Biological Macromolecules. 157,
371 687-694.
372 Wang, Z., Huang, Y., Wang, M., Wu, G., Geng, T., Zhao,Y., Wu, A. 2016
373 Macroporous calcium alginate aerogel as sorbent for Pb^{2+} removal from water media，
374 Journal of Environmental Chemical Engineering. 4, 3185-3192.
375 Wu, J., Cheng, X., Li,Y., Yang,G., 2019 Constructing biodegradable
376 nanochitin-contained chitosan hydrogel beads for fast and efficient removal of Cu(II)
377 from aqueous solution. Carbohydrate Polymers. 211, 152-160.
378 Yap, P. L., Tung, T.T., Kabiri, S., Matulick, N., Tran, D.N.H., Losic, D. 2020
379 Polyamine-modified reduced graphene oxide: a new and cost-effective adsorbent for
380 efficient removal of mercury in waters. Separation and Purification Technology 238,
381 116441.
382 Zhang, D., Xiao,J., Guo, Q., Yang, J. 2019 3D-printed highly porous and
383 reusable chitosan monoliths for Cu(II) removal, Journal of Materials Science. 54,
384 6728-6741.
385 Zhu, H., Yuan, J., Tan, X., Zhang, W., Fang, M., Wang, X. 2019 Efficient
386 removal of Pb^{2+} by Tb-MOFs: identifying the adsorption mechanism through
387 experimental and theoretical investigations. Environmental Science-Nano 6 (1),

261-272.

Zhang, W., Song, J., He, Q., Wang, H., Lyu, W., Feng, H. et al. 2020 Novel pectin based composite hydrogel derived from grapefruit peel for enhanced Cu(II) removal, Journal of Hazardous Materials 384, 121445.

Zhang, W., Song, J., He, Q., Wang, H., L, W., Feng, H., et al. 2020 Novel pectin based composite hydrogel derived from grapefruit peel for enhanced Cu(II) removal. Journal of Hazardous Materials 384, 121445.

Zhang, Q.Q., Zhu, Y.J., Wu, J., Shao, Y.T., Cai, A.Y., & Dong, L.Y. 2019 Ultralong Hydroxyapatite Nanowire-Based Filter Paper for HighPerformance Water Purification. ACS Applied Materials & Interfaces 11, 4288-4301.

Highlights

- A novel eco-friendly cross-linked HCA bio-adsorbent were prepared by a three-step method.
- The bio-adsorbent beads (HCA) showed excellent adsorption capacities for Cu(II), and the adsorption kinetics and isotherms were studied.
- Unlike traditional nanomaterials adsorbents, the spherical HCA beads, with a above diameter of 3-5mm, were easily separated after the adsorption process.
- The HCA bio-adsorbent can be easily regenerated and reused repeatedly for Cu(II) adsorption.